Electronic Supplementary Material (ESI) for Soft Matter.

Electronic Supplementary Information (ESI) for "Assembly of three-dimensional binary superlattices from multi-flavored particles"

Evan Pretti,[1] Hasan Zerze,[1] Minseok Song,[1] Yajun Ding,[1] Nathan A. Mahynski,[2] Harold W. Hatch,[2] Vincent K. Shen,[2] and Jeetain Mittal[1,*]

[1] *Department of Chemical and Biomolecular Engineering, Lehigh University, 111 Research Dr., Bethlehem, Pennsylvania 18015-4791, USA.*

[2] *Chemical Sciences Division, National Institute of Standards and Technology, Gaithersburg, Maryland 20899-8320, USA.*

* jeetain@lehigh.edu

I. SUPPLEMENTARY TEXT

A. Pair potential model

A Fermi-Jagla potential was used to model the pairwise interactions between particles. The specific functional form employed is:

$$\frac{U(r/\sigma)}{\epsilon} = \left(\frac{\epsilon_c}{\epsilon}\right)\left(\frac{\sigma_c/\sigma}{r/\sigma - R_s/\sigma}\right)^n + \frac{A_0/\epsilon}{1+\exp[A_1(r/\sigma - A_2)]} - \frac{B_0/\epsilon}{1+\exp[B_1(r/\sigma - B_2)]} \quad (1)$$

The physical effects modeled by each of the terms in this equation, as well as the influences of the individual parameters on the overall behavior of the potential, are discussed in Sec. 2.1 of the main manuscript. The parameter B_0 was adjusted between 0 and 1.3219ϵ, which varies the potential from being purely repulsive to being attractive with a well depth of ϵ, respectively. Over this range, the position of the minimum of the potential well varies between 1.0279σ and 1.0297σ. The remainder of the parameters were fixed to the following values:

$n = 36$	$\epsilon_c = 10\epsilon$	$\sigma_c = 0.2\sigma$
$R_s = 0.8\sigma$	$A_0 = 11.035\epsilon$	$A_1 = 404.40$
$A_2 = 1.0174$	$B_1 = 1044.5$	$B_2 = 1.0306$

This model is based on results from a sequence-specific model [1] for nano-scale particles. This approach has been used previously to study micron-sized particle assembly in two dimensions [2], in which it was found to yield results in agreement with experiments.

B. Common neighbor analysis (CNA)

We used common neighbor analysis (CNA) to identify and quantify the structural and compositional order of the observed crystals. We found CNA triplets and their counts for each particle in a crystal and compared them with those of reference structures. The CNA indices and their counts for finite crystals simulated with an MCJ potential are provided in Table I. The overall structure is assigned first, followed by the binary compositional order. When a particle is identified to be contained within an FCC lattice, the CNA indices of that particle with respect to its neighbors of the same type are used to further classify it as existing within a CuAu, CuPt, $AuCu_3$, $CuPt_3$ or compositionally disordered FCC structure.

Similarly, a particle in an HCP lattice is identified as HCP-straight or compositionally disordered HCP based on the CNA indices calculated for its neighbors of the same type. Likewise, BCC particles are tested to find whether or not they exist within a CsCl structure.

II. SUPPLEMENTARY FIGURES AND TABLES

A. Supplementary figures

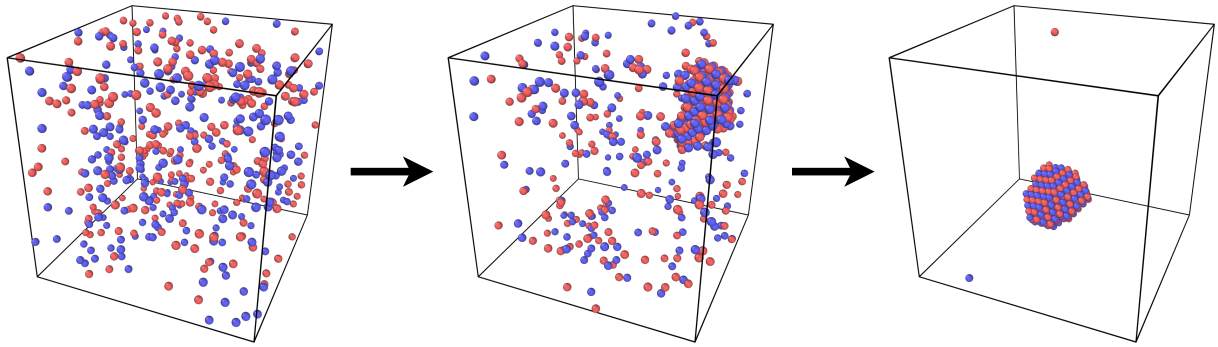

FIG. S1. Snapshots of an MD simulation at $E_{AA}/E_{AB} = E_{BB}/E_{AB} = 0$ showing (left) the initial configuration, (center) a growing crystal, and (right) the assembled crystal.

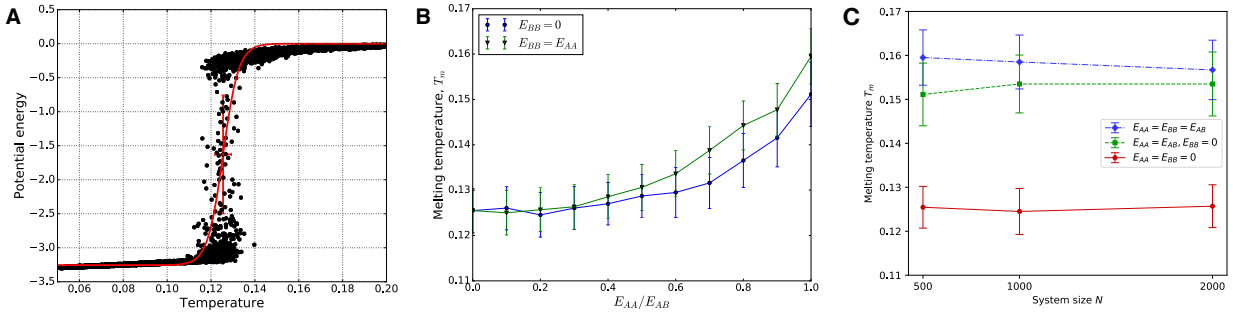

FIG. S2. A: Estimation of the melting temperature obtained from a cooling run using a sigmoidal fit to the potential energy as a function of temperature, represented for $E_{AA}/E_{AB} = E_{BB}/E_{AB} = 0$. B: The melting temperatures as a function of E_{AA}/E_{AB} for both $E_{BB}/E_{AB} = 0$ and $E_{BB}/E_{AB} = E_{AA}/E_{AB}$ cases. C: Melting temperature vs. total system size for three indicated cases.

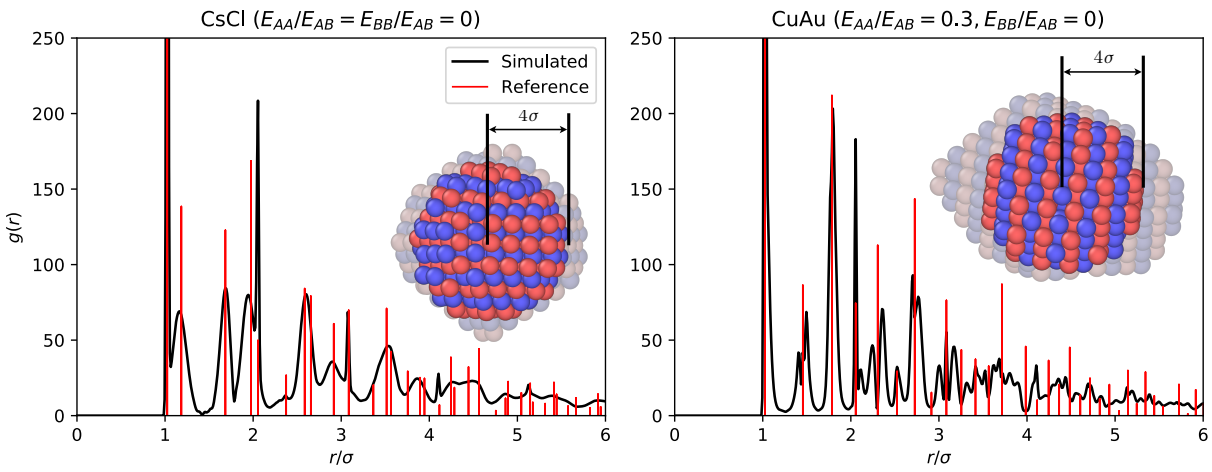

FIG. S3. Radial distribution functions (RDFs) for CsCl (left) and CuAu (right) structures averaged over 5 replicate MD simulations, compared to RDFs of perfect spherical crystallites of exactly 500 particles each. For each case, a simulation snapshot from one replicate is shown, where particles within 4σ of the center are highlighted for scale. The apparent loss of long-range order in the RDFs as r increases is not due to inherent structural disorder in the crystals, but rather, their finite sizes as illustrated by the scales in the snapshots.

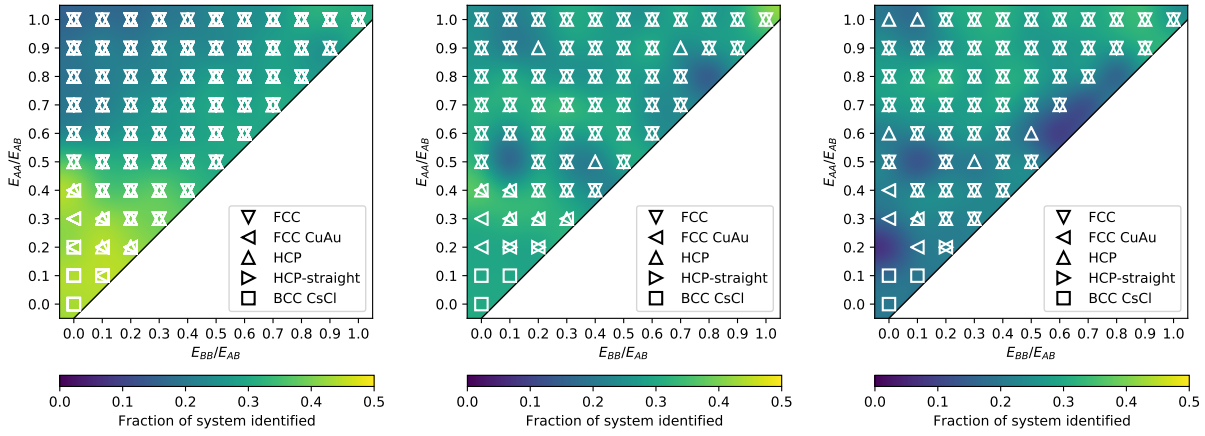

FIG. S4. The order diagram of Fig. 2 (left), compared with diagrams generated in the same manner for A:B solution stoichiometries of 2:1 (center) and 3:1 (right). In a few cases, self-assembly into ordered structures was not observed at the selected temperatures.

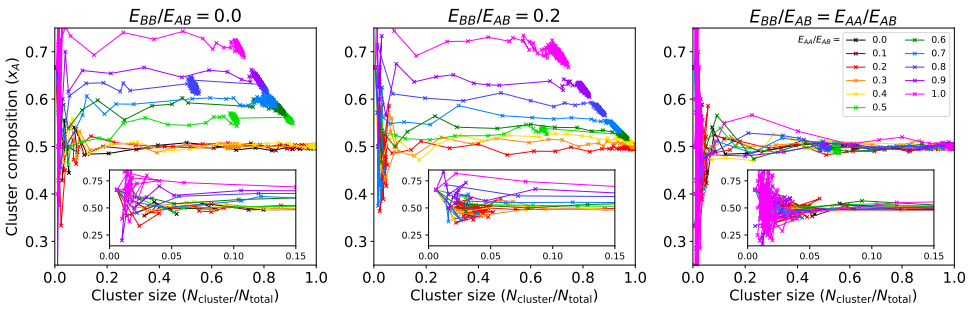

FIG. S5. Cluster composition as a function of cluster size for the simulations of Fig. 4 in the main manuscript. Each plot corresponds to one of the three cases for values of E_{BB}/E_{AB}.

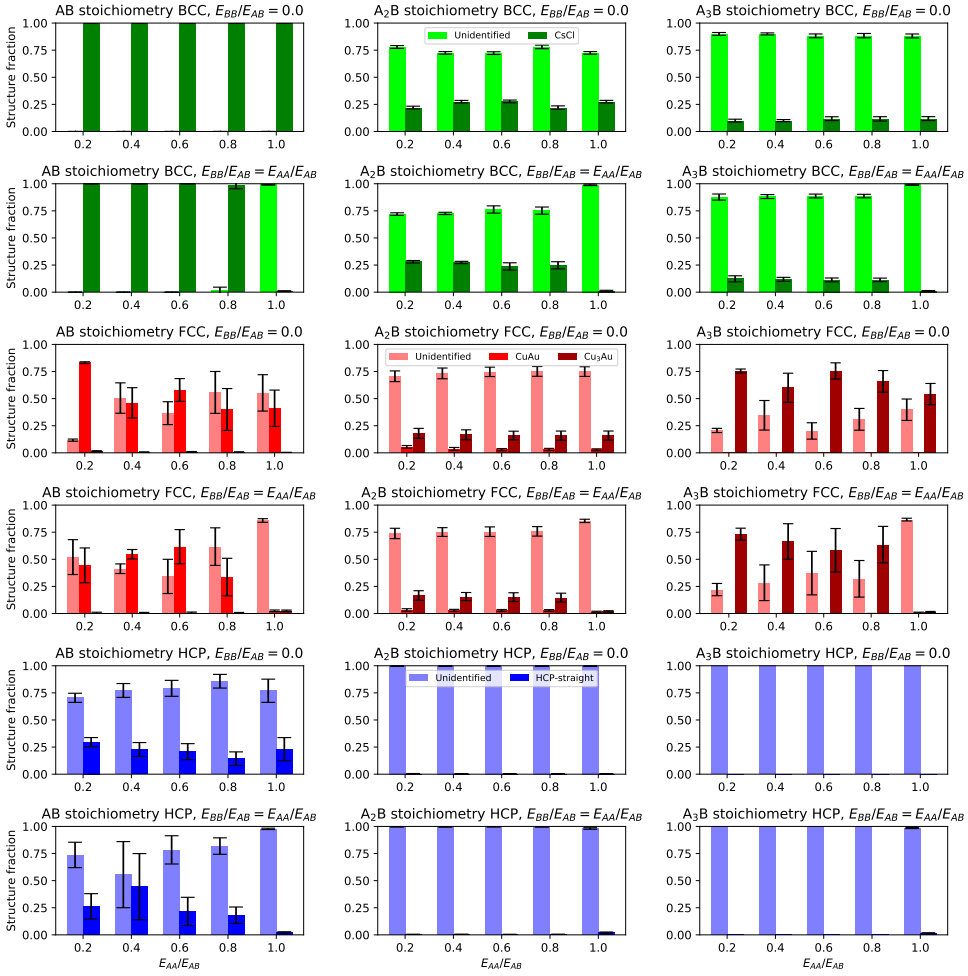

FIG. S6. Compositional order results from Wang-Landau simulations at three different stoichiometries for BCC, FCC, and HCP crystals. CuPt and Pt_3Cu were searched for in the FCC cases but not discovered in significant amounts.

B. Supplementary tables

TABLE I. List of CNA indices and the corresponding counts for the reference structures.

Crystal	R_{cut}/D_p	**CNA indices**	
		All particles	**Only A or B particles**
BCC	adaptive	$8\times(666), 6\times(444)$	—
FCC	adaptive	$12\times(421)$	—
HCP	adaptive	$6\times(421), 6\times(422)$	—
CsCl	1.40	—	$6\times(000)$ or $5\times(000)$ or $4\times(000)$ or $3\times(000)$
CuAu	1.55	—	$2\times(000), 4\times(211), 4\times(421)$ or $1\times(000), 2\times(100), 1\times(200)$ or $1\times(000), 1\times(200), 2\times(211), 2\times(311), 1\times(421)$ or $2\times(000), 1\times(200), 2\times(211), 2\times(311), 1\times(421)$ or $1\times(000), 2\times(100), 1\times(211), 2\times(311)$ or $1\times(000), 3\times(211), 2\times(311), 2\times(421)$ or $2\times(000), 2\times(100), 1\times(211), 2\times(311)$ or $2\times(000), 3\times(211), 2\times(311), 2\times(421)$ or $1\times(000), 1\times(100), 2\times(211), 1\times(311)$ or $2\times(000), 1\times(100), 2\times(211), 1\times(311)$ or $2\times(000), 2\times(100), 1\times(200)$ or $1\times(000), 4\times(211), 4\times(421)$
CuPt	1.55	—	$6\times(200)$ or $2\times(100), 2\times(200)$ or $2\times(100), 1\times(200)$ or $2\times(100)$
$AuCu_3$	1.55	—	$4\times(211), 2\times(466), 8\times(676)$ or $6\times(000)$ or $5\times(000)$ or $4\times(000)$ or $3\times(000)$ or $2\times(211), 2\times(433), 1\times(466), 2\times(543), 2\times(566), 2\times(676)$ or $3\times(211), 1\times(433), 1\times(466), 3\times(543), 1\times(566), 3\times(676)$ or $2\times(211), 1\times(311), 1\times(333), 2\times(421), 1\times(433), 2\times(543)$ or $2\times(100), 3\times(466), 2\times(566)$ or $2\times(211), 2\times(466), 4\times(566), 4\times(676)$ or $3\times(100), 2\times(466), 3\times(566)$ or $2\times(100), 2\times(333), 2\times(433)$ or $3\times(211), 2\times(466)2\times(566), 6\times(676)$ or $4\times(100), 1\times(466), 4\times(566)$ or $2\times(211), 2\times(333), 2\times(433), 4\times(543)$ or $3\times(100), 1\times(333), 3\times(433)$ or

Continued on next page

Crystal	$R_{\mathrm{cut}}/D_{\mathrm{p}}$	CNA indices	
		All particles	**Only A or B particles**
Continued from previous page			
$AuCu_3$ *(continued)*			$2\times(100), 1\times(211), 2\times(311)$ or $4\times(211), 1\times(466), 4\times(543), 4\times(676)$ or $3\times(211), 2\times(333), 6\times(543)$ or $3\times(211), 1\times(333), 3\times(421), 3\times(543)$ or $4\times(211), 4\times(421)$ or $3\times(211), 2\times(311), 2\times(421)$
$CuPt_3$	1.55	—	$2\times(211), 4\times(333), 4\times(555), 2\times(663), 2\times(677)$ or $2\times(444), 8\times(555)$ or $2\times(000)$ or $1\times(000)$ or $3\times(211), 1\times(322), 1\times(333), 1\times(444), 1\times(543), 1\times(555)$ or $1\times(100), 2\times(211)1\times(311), 1\times(322), 1\times(333), 1\times(444), 1\times(543), 1\times(555)$ or $4\times(322), 1\times(444)$ or $1\times(100), 1\times(211), 1\times(322), 1\times(333), 1\times(433), 1\times(444), 1\times(555)$ or $1\times(211), 1\times(322), 3\times(333), 1\times(444), 1\times(543), 3\times(555), 1\times(663), 1\times(677)$ or $2\times(211), 2\times(322)$ or $2\times(211), 4\times(444)$ or $2\times(211), 3\times(333), 1\times(433), 1\times(543), 4\times(555), 1\times(663), 1\times(677)$ or $1\times(100), 3\times(211), 1\times(311), 1\times(333), 1\times(433), 1\times(543), 2\times(555)$ or $2\times(311), 4\times(433), 1\times(444)$ or $2\times(211), 1\times(311), 2\times(333), 1\times(433), 1\times(543), 2\times(555), 1\times(677)$ or $2\times(100), 2\times(211), 2\times(311), 1\times(421)$ or $1\times(211), 3\times(333), 1\times(433), 2\times(444), 1\times(543), 2\times(555), 1\times(663), 1\times(677)$ or $4\times(211), 1\times(333), 1\times(433), 1\times(543), 2\times(555)$ or $3\times(211), 1\times(333), 2\times(421), 1\times(433), 1\times(543), 2\times(555)$ or $1\times(100), 2\times(211), 1\times(333), 2\times(433), 2\times(555)$ or $1\times(211), 2\times(322), 2\times(333), 1\times(433), 2\times(543), 2\times(555), 1\times(677)$ or $1\times(000), 2\times(211), 2\times(322), 1\times(433)$ or $2\times(211), 2\times(333), 3\times(433), 2\times(543), 2\times(555), 1\times(677)$ or $1\times(000), 3\times(211), 3\times(433)$ or $1\times(200), 1\times(211), 2\times(333), 2\times(433), 2\times(555), 1\times(677)$ or $1\times(000), 2\times(100), 1\times(200)$ or $1\times(211), 4\times(333), 2\times(444), 2\times(555), 2\times(663), 2\times(677)$ or $3\times(211), 2\times(333), 1\times(421), 2\times(543), 2\times(555), 1\times(677)$
HCP-straight	1.55	—	$2\times(000), 4\times(211), 4\times(421)$ or $2\times(000), 4\times(211), 1\times(421)$ or $1\times(000), 4\times(211), 1\times(421)$ or $1\times(000), 3\times(211)$ or $4\times(211), 4\times(421)$ or $4\times(211), 1\times(421)$ or $3\times(211)$

[1] Y. Ding and J. Mittal, *J. Chem. Phys.*, 2014, **141**, 184901.

[2] M. Song, Y. Ding, H. Zerze, M. Snyder and J. Mittal, *Langmuir*, 2018, **34**, 991–998.